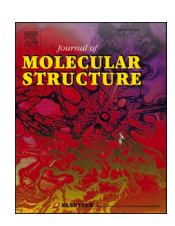
ELSEVIER

Contents lists available at ScienceDirect

# Journal of Molecular Structure

journal homepage: www.elsevier.com/locate/molstr





# Unveiling the crystal structure and quantum properties of 6-bromo-N-pyridin-4-yl-2-thiophen-2-ylquinoline-4-carboxamide: A promising journey towards predicting its anticancer potential

T.S. Shashidhara <sup>a,1</sup>, C.S. Navyashree <sup>b,1</sup>, M.K. Hema <sup>a</sup>, K. Mantelingu <sup>b</sup>, R. Jothi Ramalingam <sup>c</sup>, Muthusamy Karnan <sup>d</sup>, M. Umashankar <sup>e</sup>, N.K. Lokanath <sup>a,\*</sup>

- <sup>a</sup> Department of Studies in Physics, University of Mysore, Manasagangotri, Mysuru, Karnataka 570 006, India
- <sup>b</sup> Department of Studies in Chemistry, University of Mysore, Manasagangotri, Mysuru, Karnataka 570 006, India
- <sup>c</sup> Department of Chemistry, College of Science, King Saud University, P.O. Box. 2455, Riyadh 11451, Saudi Arabia
- d Grassland and Forage division, National Institute of Animal Science, Rural Development Administration, Chungcheongnam-do, Cheonan-si 31000, South Korea
- <sup>e</sup> Department of studies and research in Chemistry, KSOU, Mukthagangotri, Mysuru, Karnataka 570 006, India

#### ARTICLE INFO

#### Keywords: Quinoline Heterocyclic Topoisomerase Antioncogenic

#### ABSTRACT

The wide range of pharmalogical activity exhibited by quinoline derivatives, due to its fused benzene ring with pyridine structure, has made them a popular framework for medicinal chemistry. The single crystal X-ray diffraction and quantum computational studies revealed the crystal packing of the novel saturated quinoline derivative, 6-bromo-N-pyridin-4-yl-2-thiophen-2-ylquinoline-4-carboxamide. The structural examination of titled molecule unveiled the involvement of carboxyl functional group and N-heterocyclic pyridine rings in various intermolecular interactions that are responsible for upholding the crystal stability, which was validated by the Hirshfeld surface analysis. Furthermore, *in silico* studies were performed to scrutinize the antioncogenic properties of entitled molecule. Topoisomerase, a vital enzyme involved in DNA replication and repair which regulates DNA topical structure makes it a prime candidate for targeted anticancer therapies. The ligand's acceptable binding affinity to the targeted protein was identified through molecular docking, and dynamic simulation was carried out to monitor and analyse the fluctuations of ligand-protein complex for a simulation period of 100ns. Eventually, the novel molecule exhibited the most favourable interaction and stability within the substrate-binding pocket of targeted protein.

# 1. Introduction

Organic small molecules and drug candidates are of paramount importance in the field of pharmaceutical research and development. Their significance arises from their unique capability to permeate cell membranes and interact with intracellular proteins [1–3]. These molecules serve as the foundation for the development of novel therapeutic agents with diverse applications in medicine. Heterocyclic compounds, which play a vital role in the core structure of drugs [4], are particularly important in biological and pharmaceutical processes [5–10]. Quinoline stands out as one of the most important nitrogen-based heterocyclic compounds with significant biological activity. The distinctive properties of quinoline, including its enhanced basicity, hydrogen bonding

capability, and polarity, make it an attractive framework for the development of biologically active compounds. These properties allow for interactions with target enzymes, improve water solubility, and contribute to the overall effectiveness and pharmacokinetics of quinoline-based drugs [11,12]. One such compound is dihydroquinoline-4-carboxamide, an organic heterocyclic compound with the chemical formula C10H10N2O. It belongs to the quinoline compound family, which is characterized by a fused ring system consisting of a benzene and protonated pyridine ring [13]. Quinoline-based compounds have been extensively studied due to their occurrence in natural products and their diverse pharmacological effects [14,15]. They have demonstrated antimicrobial [16,17], antifungal [18,19], antiviral [20], anti-leishmanial [21], antioxidant [22,23], anticancer

E-mail address: lokanath@physics.uni-mysore.ac.in (N.K. Lokanath).

<sup>\*</sup> Corresponding author.

<sup>&</sup>lt;sup>1</sup> These authors have equally contributed to this work.

[24,25], corrosion inhibition [26,27], and antimalarial [28,29] properties, such as chloroquine and quinine. They have also shown potential as antioxidants [30], anti-SARS-CoV-2 agents [31], and DNA binders [32].

Cancer is a serious global health challenge characterized by the abnormal and uncontrolled growth of cells, leading to the formation of malignant tumours. It is the second leading cause of death worldwide, surpassed only by cardiovascular diseases [33]. The impact of cancer is significant, with nearly 600 different types of cancers identified. Each type of cancer has its own unique characteristics, origins, and response to treatment. Annually, there are approximately 14 million newly diagnosed cancer cases, resulting in the unfortunate loss of about 9 million lives [34,35]. Addressing cancer requires a comprehensive and multidisciplinary approach. This includes efforts focused on prevention, early detection, accurate diagnosis, effective treatment strategies, and supportive care. Advancements in research and understanding the underlying mechanisms of cancer are vital in developing innovative therapies that can improve patient outcomes and alleviate the burden on individuals and society as a whole. The unique heterocyclic structure of quinoline holds great significance in the field of medicinal chemistry, particularly in the development of novel anticancer agents. Quinoline-based compounds have demonstrated their potential in combating cancer through their diverse mechanisms of action and therapeutic properties. Their wide-ranging applications in medicinal chemistry open up new avenues for innovation in cancer treatment and care. By harnessing the inherent characteristics of quinoline and exploring its various derivatives, researchers can pave the way for further advancements in the development of effective therapies and strategies to combat cancer. Some of the quinoline based drugs in the markets such as, Foretinib (1), Cabazantinib (2), Lenvatinib (3), Bosutinib (4), Topotecan (5), Irinotecan (6), Belotecan (7), Neratinib (8) and Camptothecin (9) are widely used in cancer treatment [36,37]. The utility of quinoline-containing compounds extends beyond their use as anticancer drugs and encompasses various areas of medicinal chemistry.

Taking these factors into consideration, the objective of this research was to identify a potential molecule and gain a deeper understanding of its intriguing mechanism. The study aimed to investigate the potential of the molecule as an anti-cancer agent using in silico approaches. In line with these goals, a novel compound called 6-bromo-N-pyridin-4-yl-2thiophen-2-ylquinoline-4-carboxamide (BPTQC) was synthesized. This compound features a quinoline core fused with thiophene and pyridine rings at positions 2 and 4, respectively. Additionally, a bromine atom and a carboxamide functional group are attached to the fourth and sixth positions of the quinoline ring. The study utilized a detailed analysis of the crystal structure to explore the non-covalent interactions that play a crucial role in inhibiting enzymatic activity. Molecular docking and dynamic simulation analysis were employed to investigate the potential of the BPTQC molecule against specific tumour-associated proteins, leading to the conclusion that the novel molecule does indeed exhibit inhibitory properties. In summary, this study focused on the synthesis and characterization of the quinoline-based compound BPTQC. Its potential as an anticancer agent was explored using in silico approaches, including molecular docking and dynamic simulations. The results suggest that BPTQC holds promise as a potential therapeutic agent, and further experimental studies are warranted to validate its efficacy in cancer treatment.

#### 2. Materials and methods

#### 2.1. Synthesis

2.1.1. General procedure for 2-aryl substituted quinoline-4-carboxylc acidIsatin (2 millimoles) 1 was added to a solution of 2-Acetylthiophene(2 millimoles) 2 and 33% aqueous sodium hydroxide in ethanol (5 millimoles). The solution was heated under reflux in a sealed tube for 2 h. Then the reaction mixture was neutralized with sodium bisulphate

solution, resulting in the formation of a precipitate 3. The obtained precipitate was filtered and recrystallized using ethanol.

# 2.1.2. General procedure for 6-bromo-N-(pyridin-4-yl) –2-(thiophen-2-yl) auinoline-4-carboxamide

A mixture of 6-bromo-2-(thiophen-2-yl) quinoline-4-carboxylic acid 3 (1.5g, 5.4 milli moles), pyridin-4-amine 4 (1.2mL, 10 millimoles), and triethylamine (1.6mL,20 millimoles in 5.2mL of ethyl acetate (EtOAc) at room temperature was treated with T3P (6mL, 50 wt% in EtOAc, 10 millimoles) following the general procedure (Schemes 1 and 2). The coupling reaction proceeded to completion within 16 h at room temperature, resulting in the formation of amide 5. The reaction mixture was quenched with 5mL of 0.5M aq HCl solution. After diluting the mixture with 30mL of EtOAc, the phases were separated. The organic layer was washed with 20mL of 0.5M aq HCl, 20mL of saturated NaCl solution, and concentrated, yielding 2.42g of an off-white solid. Column chromatography on 80 gs of silica gel (gradient elution with a 1:1 mixture of EtOAc and hexanes) provided 2.3g of amide 3 (87% yield) as an off-white solid. <sup>1</sup>H NMR, 13C NMR and FTIR Spectra of synthesized compound are given in the supplementary Figures S1, S2, and S3.

#### 2.2. Single crystal X-ray structure determination

Suitable defect free single crystal of BPTQC was selected for data collection. X-ray intensity data were collected using Rigaku XtaLAB mini CCD diffractometer with X-ray generator operated at 50kV and 12mA, using radiation source Mo-K $\alpha$  of wavelength 0.71,073Å, keeping scan width of 0.5° and exposure time of 3s with the sample to source distance of 50mm. A complete data was processed and absorbed using CRYSTALCLEAR [38]. The structure was solved by the use of SHELXS which involves direct methods and refined by full matrix least square on  $F^2$  using SHELXL [39,40] program as implemented in OLEX2 [41] software. All the non hydrogen atoms were revealed in the first Fourier map. Various geometrical parameters were calculated using PLATON [42], ORTEP and other diagrams were generated using MERCURY software [43]. The single crystal data and structure parameter information's for BPTQC are tabulated in Table 1.

#### 2.3. Hirshfeld surface analysis

Hirshfeld surface (HS) analysis and their associated two-dimensional fingerprint plots which describe the various intermolecular interactions were generated for BPTQC using Crystal Explorer software [44]. HS analysis is mapped with normalized contact distance ( $d_{\rm norm}$ ), defined in term of nearest internal ( $d_{\rm i}$ ) and external distance ( $d_{\rm e}$ ). The HS study enables the illustration and quantification of intermolecular interactions of complex by various colours (red-blue). High resolution molecular hirshfeld surfaces,  $d_{\rm norm}$  and shape index functions were generated for BPTQC molecule using a crystallographic information file (cif). The 2-D fingerprint plots were generated by summing  $d_{\rm i}$  and  $d_{\rm e}$  obtained from the 3-D Hirshfeld surface meanwhile, the percentage contribution of intermolecular interactions was also obtained.

## 2.4. Density functional theory

Density functional theory methods were used to calculate the quantum mechanical ground state energy of the molecule and to analyse the electronic structure of the system using *Gaussian 16* software [45, 46]. The electron density function was obtained from an initial approximation of single crystal X-ray diffraction (cif) to compute the electron wave functions. Using the optimised electron density wave function, various physical and chemical properties can be predicted. Koopman's approximation and density of states was used to calculate the energy difference between two molecular orbitals. MEP analysis was carried to determine the electrostatic potential of the molecule. Furthermore, non-covalent interaction (NCI) and electron charge

Scheme 1. Synthesis of 2-aryl substituted Quinoline-4-carboxylc acid (3).

Scheme 2. Synthesis of 6-bromo-N-(pyridin-4-yl)-2-(thiophen-2-yl) quinoline-4-carboxamide (5).

**Table 1**Crystal data and structure refinement parameters.

Parameter	Values
CCDC Number	2,267,559
Empirical formula	$C_{21}H_{20}BrN_3O_2S_2$
Formula weight	490.43
Crystal system	monoclinic
Space group	$P2_1/n$
Temperature (K)	293
Wavelength (Á)	0.71073
a (Å)	8.297 (3)
b (Å)	15.5200
c (Å)	16.8120
β (°)	97.4200
Volume(Á <sup>3</sup> )	2146.7 (8)
Z	4
Density (Mg $m^{-3}$ )	1.517
$\mu  (\text{mm}^{-1})$	2.132
$F_{000}$	996
Final $[I > 2\sigma(I)]$	R1=0.1145, wR2=0.2968
R indices (all data)	R1 = 0.2295, wR2 = 0.3734
Reflections collected	10,879
Independent reflections	4828
Index ranges	-10≤ <i>h</i> ≤6
	$-19 \le k \le 20$
	$-21 \le l \le 19$
$\theta$ range for data collection (°)	3.18 to 27.48
Largest diff. peak and hole (e $Å^{-3}$ )	2.030 and -1.194

distribution calculation was done by *multiwfn* 3.7 software [47] and visualised by visual molecular dynamics (VMD 1.9.3) [48].

# 2.4. In silico studies

#### 2.4.1. Molecular docking

Molecular docking studies were carried out in order to investigate the binding affinity of novel molecule with 4GOU protein with the utilisation of MGL tools 1.5.6 [49] along with Auto dock vina [50,51] From the protein data bank the three dimensional structures of 4GOU protein was downloaded in PDB format and inbound ligands were untied from

protein using BioviaDiscoveryStudio visualize [52]. A novel quinoline derivative was docked into the active site of 4GOU protein using Auto dock tool, negative binding affinity was obtained for docked complex in the unit of kcal/mol. The obtained protein-ligand complex wasa visualized, ligand interaction and binding sites were analysed using BioviaDiscoveryStudio visualizer.

# 2.4.2. Molecular dynamic(MD) simulations

MD simulations of 4GOU – BPTQC compound was carried out inorder to determine the DMC stability with the targeted protein using the academic version of Desmond modules in the Schrodinger 2020–2 suite [53]. With the better docking result MD simulation was performed by inundating cubic box with TIP3P water molecules, the system was solvated and the OPLS3 force filed was used to prepare and evaluate the complex. The complex in neutral system was introduced eith the use of complex algorithm, later with Marlyna-Tobias-Klein, relaxed system was subjected to 100ns simulations with 1bar pressure and Nose-Hoover thermostat set to 300K under NPT ensembles. With the use of root mean square deviation (RMSD), root mean square fluctuations (RMSF) and hydrogen bond fingerprint profile the protein-ligand energy potential stability was investigated.

# 3. Results and discussion

#### 3.1. Single crystal X-ray structure analysis

Single crystal structural studies provide precise three-dimensional information, enabling in-depth exploration of non-covalent interactions. They facilitate a comprehensive understanding of the properties and behaviours of substances by unravelling intricate details. These studies are essential for elucidating the role of non-covalent interactions in various systems [54–60,55,61,62]. The three dimensional arrangement of atoms within a crystal structure of BPTQC was determined by the single crystal X-ray diffraction technique. With the aid of single crystal analysis it was confirmed that the molecule crystallized in monoclinic crystal system with space group of  $P2_1/n$  consisting tetra molecules in each unit cell (Z=4). The ORTEP of the novel molecule with

thermal ellipsoids drawn at 50% probability level is shown in Fig. 2a and crystal data refinement parameters are depicted in table 1. The crystal structure of BPTQC contains regions of disordered solvent and mosaicity in a crystal lattice. And also the crystal size was too small, which cause the weaker diffraction signal due to limited scattering power. These factors lead to quite higher R-value (Table 1) of BPTQC molecule. The molecule exhibits a pronounced non-planar nature, with the thiophene and quinoline rings lying in the same plane (highlighted in pink in Fig. 1b). However, the pyridine ring deviates from this plane (highlighted in yellow in Fig. 1b), forming an inter-planar angle of 60.51° The thiophene ring demonstrates torsional motion involving the C11 and C12 atoms, leading to an average deviation of 0.199Å. Additionally, the S1 and Br atoms deviate from the plane by distances of 0.206Å and 0.131Å, respectively. Furthermore, the O1 atom exhibits a deviation from the plane with a distance of 0.070Å, as depicted in Fig. 2b. The presence of this tensional twisting can significantly impact the molecule reactivity, electronic properties, and biological activity.

The crystal lattice of the novel structure showcases a variety of interactions, comprising intra and intermolecular hydrogen bonds, short contacts,  $C-O\cdots\pi$  interactions and  $\pi\cdots\pi$  stackings. All these interactions

are essential in predicting and explaining the behaviour of molecule since they play vital role in molecular stability and packing. Potential hydrogen bonds and  $\pi \cdots \pi$  interactions are tabulated in Table 2. The molecule displays S(6), S(4) and S(5) synthons, formed by intra molecular hydrogen bond interactions within the molecule as illustrated in Fig. 3a.

Donor and acceptor regions in a ligand are integral components in drug design, governing its interaction with the target protein or receptor. These regions fulfil distinct functions by facilitating specific intermolecular interactions that greatly influence the ligand's binding affinity and selectivity. X-ray structure analysis provides a comprehensive understanding of the donor and acceptor regions in molecules. Fig. 3b illustrates the extensive exploration of donor and acceptor sites within the BPTQC molecule, highlighting their involvement in various intermolecular interactions. Adjacent molecules are intricately connected through non-classical hydrogen bond interactions, exemplified by the C8-H8···N3 interaction that forms a supramolecular ring motif known as  $R_2^2(18)$ . Furthermore, neighbouring molecules exhibit  $R_2^1(7)$  ring motifs as a result of H11-C11···N3, N2-H2···O2 and H19-C19···O2 interactions, effectively packed on both sides of the  $R_2^2(18)$  synthon. This

Fig. 1. The structure of some approved drugs containing quinoline as their core ring.

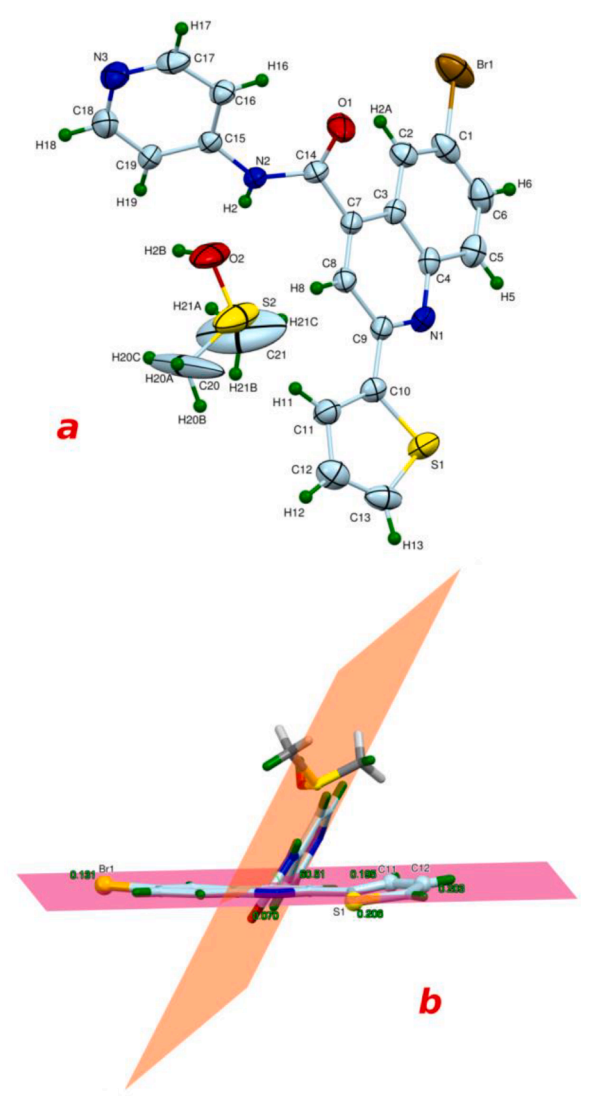


**Fig. 2.** *ORTEP* of novel molecule with thermal ellipsoids drawn at 30% probability (a) and the molecule displays a significant degree of non-planarity, with the thiophene (b).

arrangement leads to the *trans* orientation of the neighbouring molecules with respect to each other, establishing a distinct structural organization (Fig. 4a).

In addition, the BPTQC molecule exhibits two distinctive supramolecular architectures, namely  $R_1^4(26)$ ,  $R_1^2(6)$  and  $R_1^4(23)$ , positioned on either side of the  $R_2^2(18)$  architecture. These unique arrangements arise from the interactions between the DMSO solvent and neighbouring molecules. These interactions involve classical hydrogen bonding (N2-H2···O1), non-classical hydrogen bonding (H20B-C20···O1 and C21-H21C···Br1), as well as short-contact hydrogen bonds (C18-H18···H2B). These interactions are illustrated in Figs. 4b and 5a, depicting the intricate supramolecular structure formed by the BPTQC molecule.

Apart from hydrogen bond interactions,  $\pi\cdots\pi$  stacking interactions play a significant role in stabilizing ligand-protein complexes and can be utilized strategically in drug design to improve the potency and efficacy of the drug candidate. The  $\pi\cdots\pi$  donor and acceptor region in a molecule typically consists of aromatic rings or conjugated systems that can donate/accept pi-electrons. These  $\pi$ -electrons can interact with the  $\pi$ -electrons of aromatic amino acids or other  $\pi$ -donor/acceptor regions in the target protein.

BPTQC molecule exhibits the C14-O1···Cg1 interaction (Fig. 3b) and  $\pi \cdot \cdot \pi$  stackings interactions, such as Cg4···Cg2, Cg2···Cg4, Cg3···Cg3,

Cg4···Cg4 and Cg1···Cg3 interactions between the adjacent molecules (Fig. 5b and Table 2), where Cg1, Cg2, Cg3 and Cg4 are the centroids of thiophene, pyridine nitrogen (N2), pyridine nitrogen (N3) and chlorophenyl rings respectively, indicates presence of numerous the  $\pi$ -donor/acceptor regions. The distance between aromatic ring centroids is a crucial factor for assessing the strength of  $\pi$ - $\pi$  stacking interactions. An optimal range of 3.5 to 7Å indicates favourable interactions, with smaller distances indicating stronger interactions. The angle between the normal vectors of aromatic rings is also important, with an ideal angle of approximately 0° or 180° corresponding to parallel or nearparallel alignment. Deviations from this ideal angle can still support significant stacking interactions, particularly if the distance between the rings falls within the favourable range.

The presence of these various interactions, supramolecular synthons, and ring motifs due to various  $\pi\cdots\pi$  stacking contributes to overall crystal organization and plays a crucial role in enhancing the molecule stability of crystal structure, and may offer insights into the biological properties of the novel compound.

#### 3.1.1. Molecular electrostatic potential (MEP) analysis

Molecular electrostatic potential (MEP) is a representation of the electrostatic potential around a molecule or a molecular system. MEP can be used to visualize the regions of high and low electron density and to study the reactivity and properties of molecules. MEP analysis is a valuable tool in drug design as it enables the rational design and optimization of drug candidates with improved binding affinity, selectivity, and therapeutic efficacy. By understanding the electrostatic properties and interactions of molecules, can make informed decisions and develop more effective drugs with desired pharmacological properties. The MEP of BPTQC molecule depicted in the Fig. 6a. The regions that are covered by red colour around the carbonyl group are indicated as negative electrostatic potential which reflects the acceptor site of oxygen atom. The nucleophilic sites or positive electrostatic potential are shown by blue coloured regions all over the protonated hydrogen atoms of the molecule indicating the high tendency donor regions to nucleophilic attacks. Whereas green coloured surface near the aromatic rings (thiophene and N1 pyridine and benzene rings of quinoline group) of the molecule covers the  $\pi \cdots \pi$  systems, and the yellowish region around the halogen atom (bromine atom) represents that it is electro passive in nature.

#### 3.1.2. Non-covalent interactions (NCI)

Non-covalent interaction analysis, coupled with Reduced Density gradient (RDG) analysis, explores the intricate network of non-covalent interactions within molecule. The three dimensional visualization of non covalent interactions with isosurface value of 0.65 is shown in the Fig. 6b. The isosurface with red colour at the centers of benzene, pyridine and thiophene and quinoline rings indicates the impact of ring strain on molecular interactions (strong steric effect) within the molecule. The partially green-brown colour discs between carbonyl oxygen, amine group and hydrogen atoms of quinoline, benzene and thiphene rings (O1···H2A-C2, O1···H16-C16, H2···H18) represents the major intramolecular hydrogen bonds and Van der Waal weak interactions arises due to temporary dipoles formed as a result of electron cloud fluctuation.

The graphical visualization of the correlation between RDG and electron density functions as intensity of interaction. The ( $\lambda 2$ ) acts as differentiating sign between the interactions. The region with value of  $\lambda 2 < 0$ , scattered in green colour reflects the bonding (attractive) type of interaction,  $\lambda 2 > 0$  red colour region indicates non bonding or repulsive type of interaction and  $\lambda 2 \approx 0$  is identifies the Van der Waal type of interactions (Fig. 6c). The occurrence of sharp gradients in the region of low density signifies the presence of hydrogen bonding within the molecule.

**Table 2**Potential hydrogen bond and short ring interactions.

Potential Hydrogen B	onds					
Donor-HAcceptor	D-H	(Å) H···A (Å)	D…A (Å)		D-H···A (°)	Symmetry
N2-H2···O2	0.69	2.14	2.803(7)		162(7)	
C16 -H16···O1	0.93	2.28	2.861(10)		120	
C13-H13O2	0.93	2.55	3.457(12)		165	-1/2+x,3/2-y,1/2+z
C20-H20B···O1	0.96	2.40	3.344(17)		168	1/2+x,3/2-y,1/2+z
Short Ring and C-O···	Cg interactions.					
Cg(I)	Cg(J)	Cg(I)- $Cg(J)$ (Å)	α (°)	β (°)	γ (°)	Symmetry
Cg1	Cg3	4.766(6)	51.2(5)	40.8	25.5	-1/2+X,3/2-Y,1/2+Z
Cg1	Cg3	5.529(6)	51.2(5)	38.9	67.9	1/2+X,3/2-Y,1/2+Z
Cg2	Cg2	5.674(5)	5.86	0.0(4)	51	-X,2-Y,1-Z
Cg3	Cg1	4.767(6)	0.27	6.38	51.2(5)	1/2+X,3/2-Y,-1/2+Z
Cg3	Cg3	3.952(5)	4.9	0.0(5)	26.8	-X,1-Y,1-Z
Cg4	Cg4	3.666(6)	5.77	0.0(5)	8	1-X,2-Y,1-Z
Cg4-	Cg5	5.763(5)	-1.68	0.7(4)	48.3	1-X,2-Y,1-Z
Cg5-	Cg4	5.764(5)	-1.71	0.7(4)	47.8	1-X,2-Y,1-Z
C14-O1	Cg1	3.904(10)			8.95	-1/2+X,3/2-Y,-1/2+Z

Cg(I) and Cg(J) centroids of the rings, Cg(I)-Cg(J)-Centroid distance between ring I and ring J, Alpha- Dihedral angle between mean planes I and J, Beta- Angle between the centroid vector  $Cg(I) \cdots Cg(J)$ , the normal to the plane (I), Gamma- Angle between the centroid vector  $Cg(I) \cdots Cg(J)$  and the normal to the plane (J), and Slippage-Distance between Cg(I) and Perpendicular Projection of Cg(J) on Ring I (Ang).

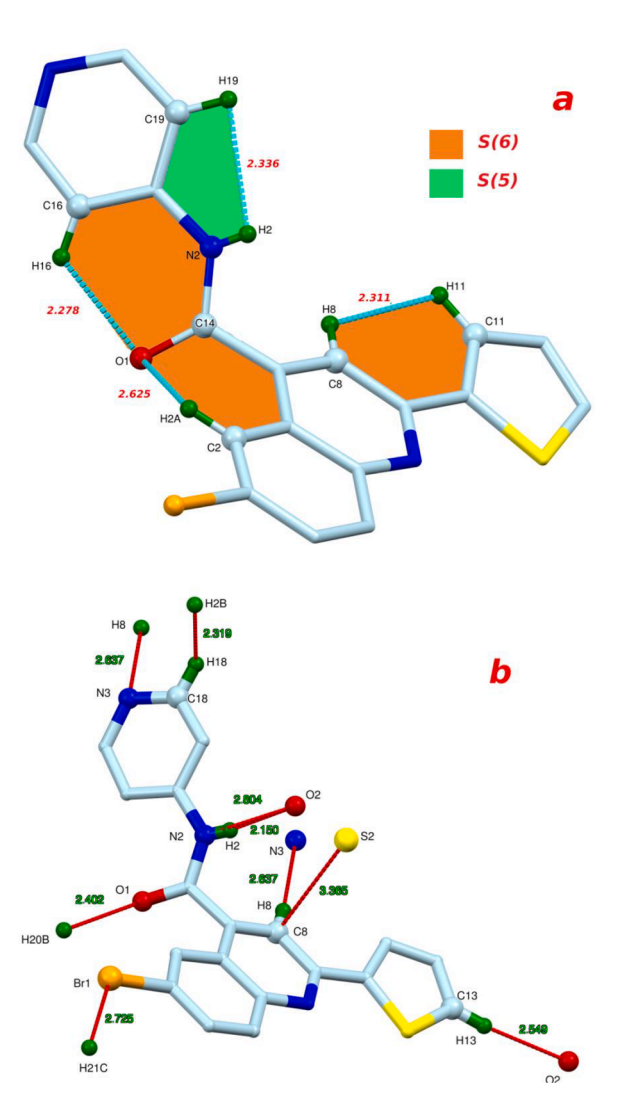


**Fig. 3.** Supramolecular ring motifs formed by intramolecular interactions within the molecule (a) and Intermolecular donor acceptor regions (b) surrounding the CPQTC molecule.

#### 3.2. Hirshfeld surface analysis (HSA)

In order to gain better understanding the stacking arrangement of molecules, it is crucial to get sight into the intermolecular interactions that are involved. Hirshfeld surface analysis is potential technique for investigating these intermolecular interactions. With the aid of crystallographic information file the HSA reflected numerous red spots on  $d_{\text{norm}}$ surface confirming intermolecular hydrogen bond interactions. The dark red region around the oxygen atoms of carbonyl and DMSO solvent confirms the presence of C20-H20B···O1 and N2-H2···O2 hydrogen bond interactions, bright red spot around the bromine atom indicates the electronegative region by confirming the C21-H21B···Br1 hydrogen bond with a bond distance of 2.975Å. Whereas light red circles near the H21A, H20B, H20C, and H20C atoms reflects the various non classical and short contacts which are mainly involved in the formation of distinct supramolecular synthons such as  $R_2^1(7)$ ,  $R_2^2(18)$  (Fig. 7a). The triangular shaped yellowish-red patches on phenyl, thiophene and pyridine rings of the novel compound spotted on shape index surface, corresponds to the Cg...Cg stackings (Table 2 and Fig. 7b). These numerous stacking interactions are also demonstrated by the relatively flat green regions separated by the dark blue boundaries on the Hirshfeld spotted on the curvedness surface around each rings of the entitled novel compound (Fig. 7c). The corresponding 2D fingerprint plot analysis exhibits the various intermolecular interactions with their percentage contribution to the total HS along with the labelled intermolecular contact values (Fig. 7d). The single prominent characteristic long spike in the 2D plot of BPTQC molecule represent the most dominating H···H interactions, with the% contribution of 41.2 to the total HS. The second most contribution to the crystal packing is from C···H/H···C contacts comprising 12.2% which appears as a broad distribution in FP plot (Fig. 7d). N···H/H···N interaction stands next to carbon-hydrogen interaction with the 9.6% of total interactions. The next highest contribution is from the halogen hydrogen interactions in the crystal showing two distinct long spikes at  $d_e + d_i \sim 1.7$ Å. Other interactions next to Br···H is of order H···S/S···H > O···H/H···O > C···C > and Br···C/C···Br also significantly contribute to the overall stability of the crystal structure (Fig. 7d).

#### 3.3. Molecular docking

Molecular docking stands out as a highly effective computational technique for predicting the interaction between drug molecules (ligands) and biological macromolecule (protein, nucleic acid or other molecule). This involves predicting the binding mode and affinity of ligand to protein. This employs in identifying optimal orientation and

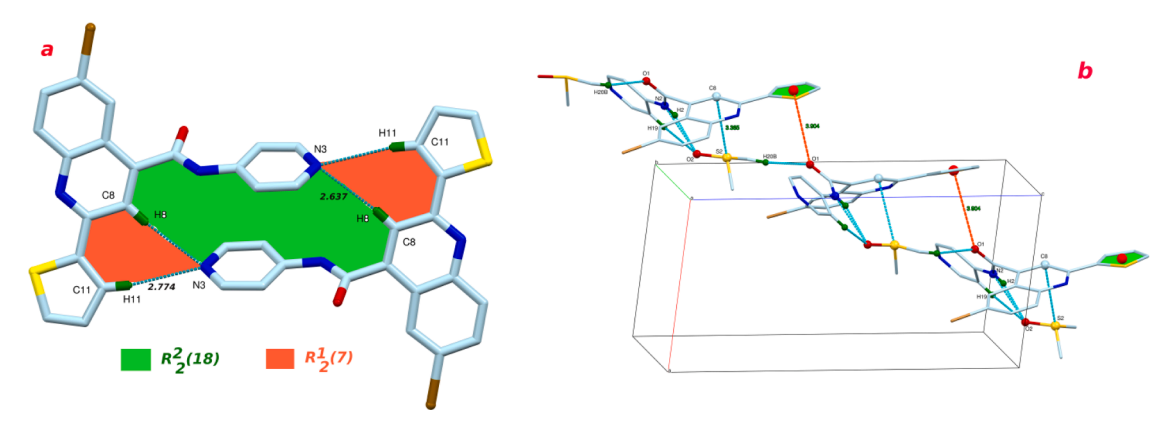


Fig. 4. Intermolecular (a) C11-H11 $\cdots$ N3 and C8-H8 $\cdots$ N3 interactions resulting Supramolecular architectures and Molecular packing (b) due to intermolecular C-O $\cdots$ Cg interaction (red colour dotted lines).

conformation of ligand within the binding site of protein, such that binding energy is minimized. The molecular docking of novel BPTQC molecule is investigated with the Auto dock vina and Biovia Discovery Studio tools.

By analysing the molecular docking of BPTQC with topoisomerase protein (PDB ID: 4GOU), a highly favourable binding site was identified with a binding score of -7.4kcal/mol. Cartoon and surface representation of protein with the ligand docked inside the active site is shown in the Fig. 8a and 8b respectively. Table 3 sums up the different types of bonding profiles towards the active site of the targeted protein, indicating that synthesized novel molecule exhibits high affinity towards various amino acids such as TYR327, THR334, ALA337, ASP179 and PHE330 of the topoisomerase, characterized by various types of

interactions displayed in Fig. 9. Additionally, the ligand-protein interactions are consistently governed by the atoms of intermolecular  $\pi\cdots\pi$  interaction, which also participated in constructing various supramolecular motifs in the molecule's crystal packing. Sigma··· $\pi$  and Anion··· $\pi$  interactions facilitate the interaction of thiophene ring and pyridine ring with N3 nitrogen atom of ligand with the topoisomerase protein with catalytic residues comprising THR334 and ASP179, with bond distance of 3.76 and 3.79Å, respectively. Furthermore, analysis indicates that the halogen group present in the ligand (BPTQC) molecule interact with the PHE330 and TYR327 residues of the protein, demonstrating the strong binding affinity of the ligand to the catalytic site of targeted protein by  $\pi$ ····alkyl type of interactions (Fig. 9 and Table 3). Moreover, thiophene ring and benzene ring of quinoline group interacts with ALA337 and

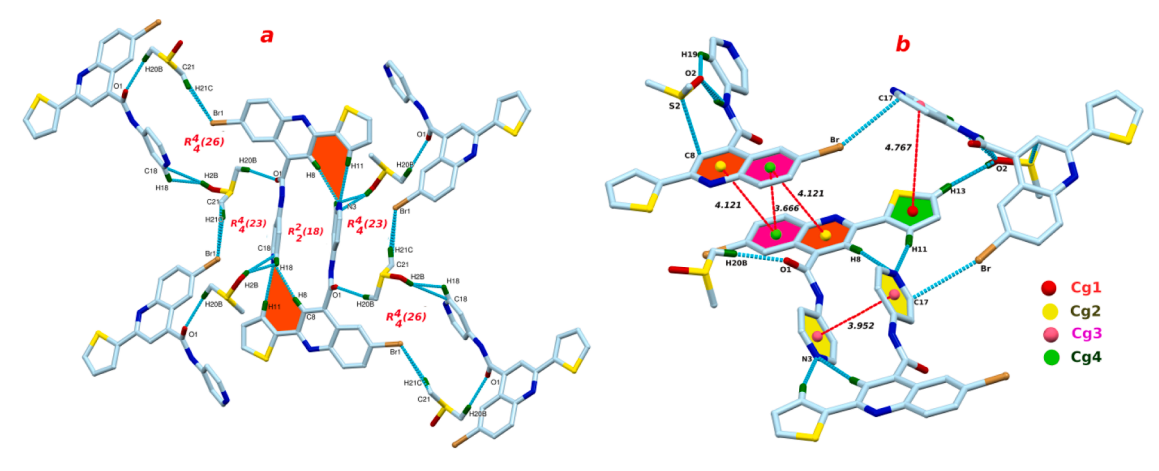


Fig. 5. Supramolecular synthons (a) formed due to intermolecular hydrogen bond interactions and Cg...Cg stacking interactions (b) between the adjacent CPTQC molecules.

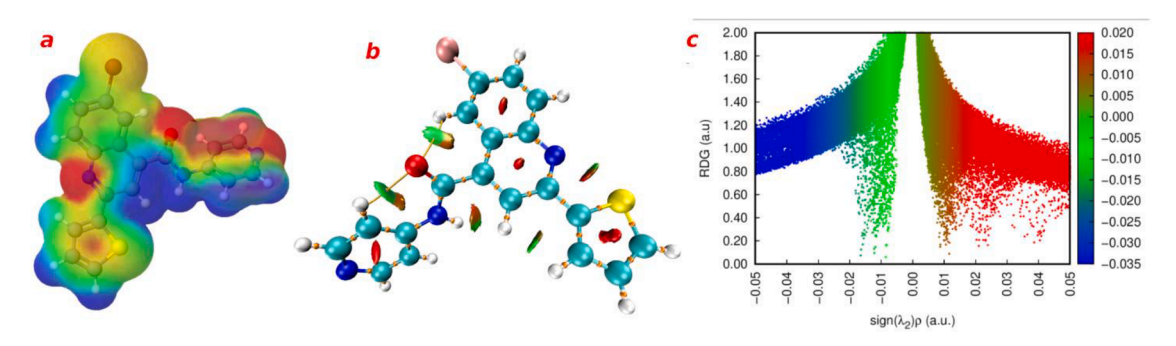


Fig. 6. Molecular electrostatic graph (a), Non-covalent intra molecular interaction with isosurface value of 0.65 (b) and 2D RDG scatter graph (c) of quino-line derivative.

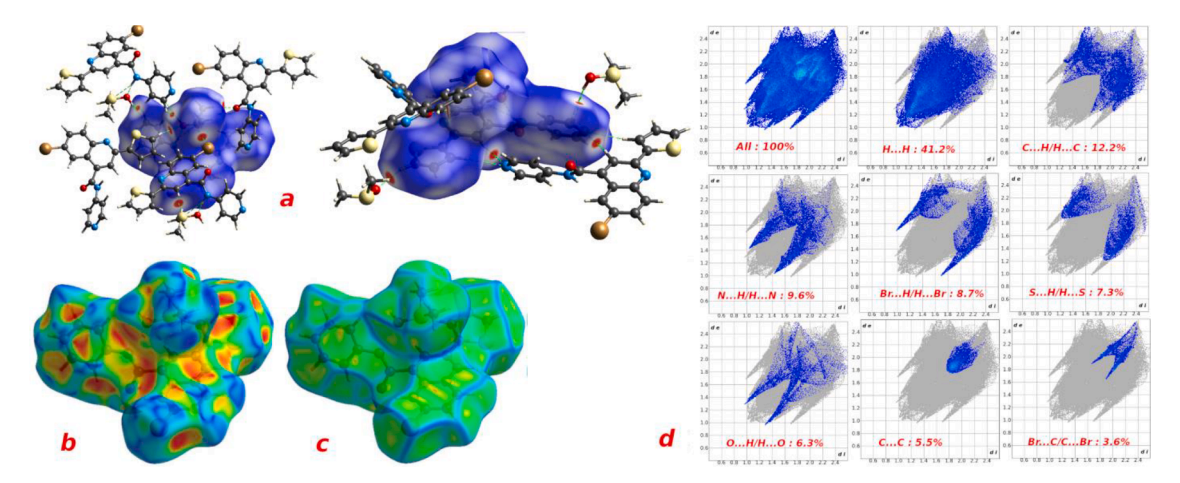


Fig. 7. 3D Hirshfeld surfaces mapped with  $d_{\text{norm}}$  (a) shape index (b) curvedness (c) and 2D fingerprint plots (d) of BPTQC molecule. Resolved contacts showing the percentages of contacts contributed to the total Hirshfeld surface.

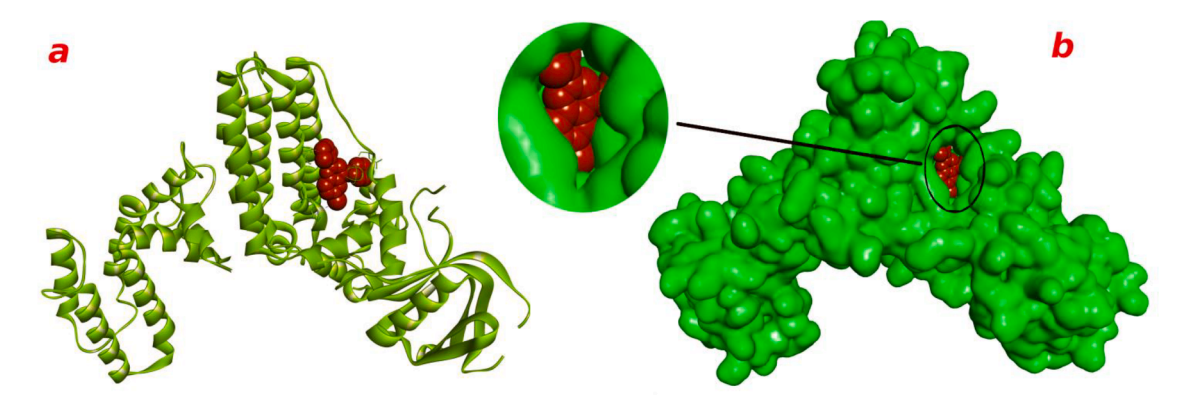


Fig. 8. Novel compound docked with topoismerase (PDB: 4GOU): Cartoon (a) and surface (b) representation of ligand in the active site.

TYR327 amino acids of 4GOU through  $\pi$ ···alky and  $\pi$ ··· $\pi$  interactions, respectively.

## 3.4. Molecular dynamic simulation

can be utilized as a robust approach to examine the stability of the ligand-protein complex in order to gain much more insights into the outcomes of molecular docking. It is an effective method to assess the complexes ability to maintain their conformation and adaptability was examined by analysing various parameters, including root mean square deviation (RMSD) and root mean square fluctuation (RMSF) of the ligand-protein atoms throughout the certain simulation period of 100ns. The complex allowed running for a simulation span of 100ns, the RMSD and RMSF measurements are depicted in Figs. 10 and 11.

# 3.4.1. RMSD

Root mean square deviation provides valuable information about average distance and fluctuation of molecule within the complex, which determines the stability and structural conformational changes of

**Table 3** Interaction of title compound with main protease through spike binding domain.

Protein(Amino acids)	Ligand	Interaction type	Bond distance (Å)
TYR327 THR334 ALA337 ASP179 PHE330	π of benzene π of thiophene π of thiophene N3 of Pyridine Br	π - π T-shaped π - Sigma π - Alkyl π - Anion π - Alkyl	4.95 3.76 5.43 3.79 5.24
TYR327	Br	π - Alkyl	5.29

complex during the simulation. The RMSD graph of BPTQC molecule reveals a remarkable stability of ligand throughout the simulation, with very minimal deviation of  $\sim 1 \mbox{\normalfont A}$  observed between 45–50 nanoseconds (ns). Apart from this short interval, ligand maintains a consistently stable binding affinity to the catalytic site of the protein. This consistently low deviation reflects its stabilized conformation throughout the simulation as observed in Fig. 10a, highlighting the ligand's potential for effective binding and therapeutic activity.

In contrast to the ligand, protein exhibits a higher deviation, as observed in the protein RMSD plot Fig. 10b. Initially, the RMSD of the protein gradually increases, reaching a deviation of  $\sim\!\!2$  to 3.7Å within the first 20ns of the simulation. However, after this initial period, the protein stabilizes, with the deviation decreasing to  $\sim\!\!1.3$ Å and remained relatively constant upto 40ns mark. From there on, the protein maintains stability, with the deviation decreasing further to less than 1Å until the end of the simulation. These observations indicate that the protein initially underwent structural adjustments and conformational changes, but eventually attained the relatively stable state as the simulation progressed.

#### 3.4.2. RMSF

Using root mean square fluctuations we were able to evaluate the extent of fluctuation and dynamic behaviour exhibited by each amino acid within the protein structure during the simulation (Fig. 11a). Throughout the simulation duration, a detailed analysis was conducted to further comprehend the protein's flexibility. This involved calculating the average root mean square fluctuation (RMSF) values for each amino acid in the 4GOU protein while considering the presence of the BPQTC molecule. The resulting RMSF plot revealed that the binding process

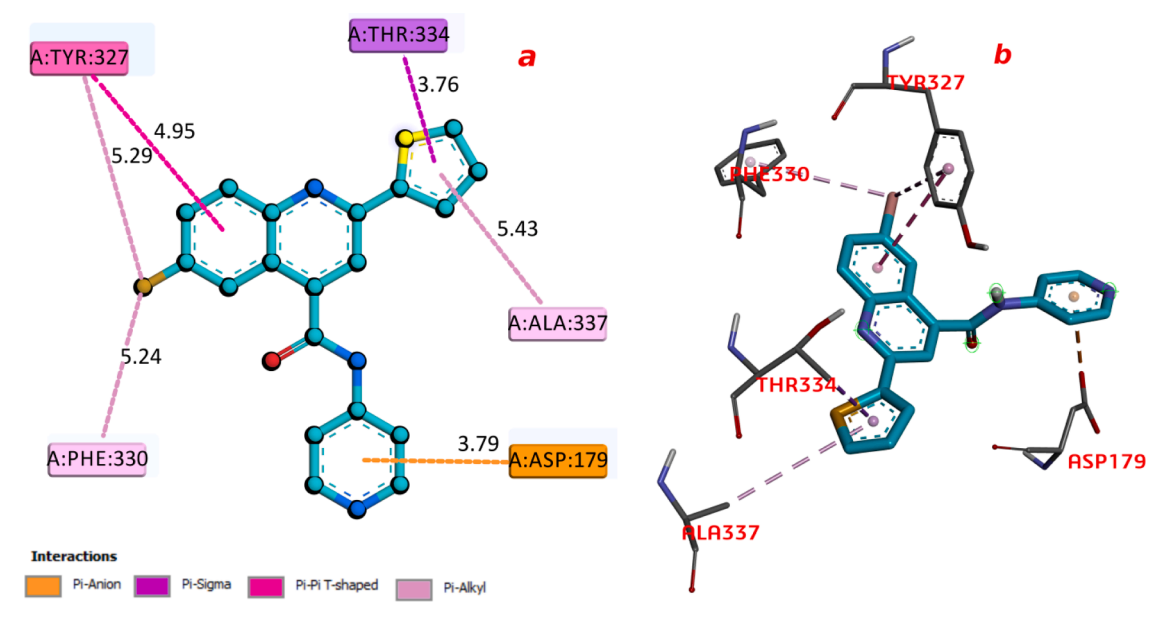


Fig. 9. 2D (a) and 3D (b) representation highlighting interaction of novel quinoline derivative with targeted protein.

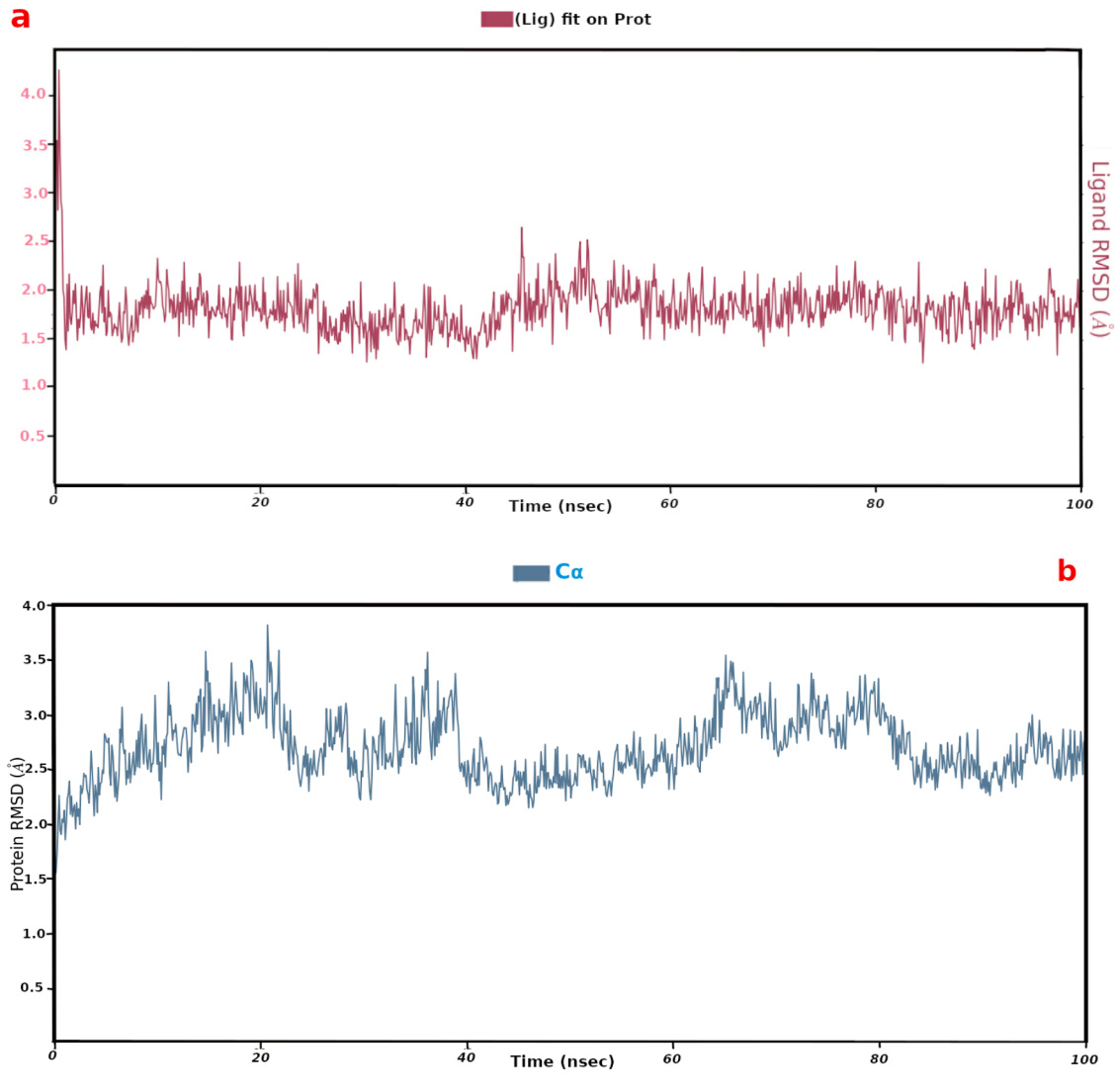


Fig. 10. RMSD plot of ligand (a) and protein (b) reflecting the deviations during the simulation span of 100ns.

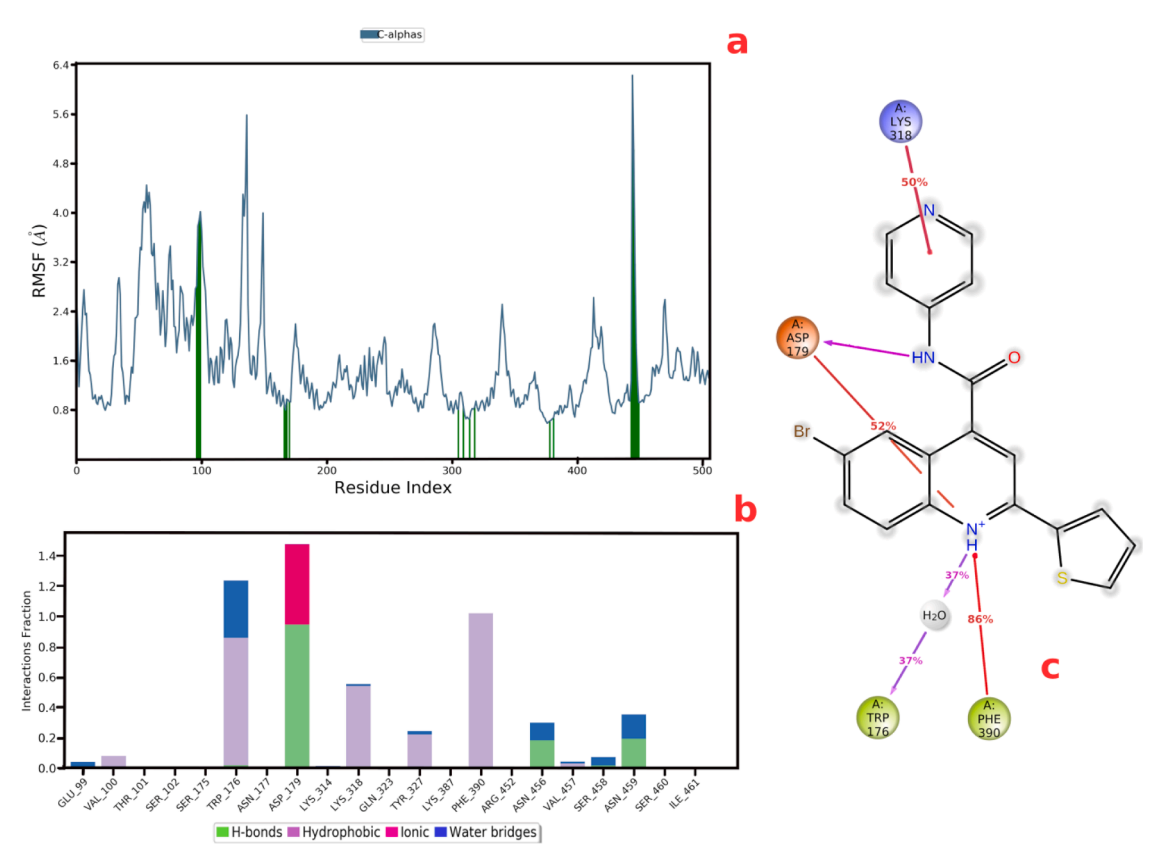


Fig. 11. RMSF graph (a) representing dynamic behaviour of active site amino acids, protein-ligand interactions depicted in 2D histogram plot (b) and 2D ligand-protein contacts (c).

with the receptor remained stable, exerting a negligible impact on the protein's flexibility during the entire simulation period. The residues that exhibited highest fluctuations in the RMSF plot were identified as SER98 (2.77Å), VAL100 (3.79), THR101 (3.88), SER102 (4.02), ASN456 (6.23), VAL457 (5.02), SER458 (3.17). These residues exhibited relatively greater flexibility, possibly due to their locations within the protein structure. These regions are corresponding to flexible loops or protein termini province. The catalytic site residues SER175 (0.90), TRP176 (0.80), ASN177 (0.99), ASP179 (0.93), GLN313 (0.82), LYS318 (0.85), GLN323 (0.66), PHE390 (0.67), LYS387 (0.62), LEU389 (0.66), ARG452 (1.27), ASN459 (1.87), SER460 (1.28) and ILE461 (0.92) are interacted with the ligand with minimal fluctuations as in the RMSF plot. These specific residues were identified and marked with vertical green-colour lines to highlight their involvement in the protein-ligand binding (Fig. 11a).

# 3.4.3. Protein-ligand interactions

The study of protein-ligand interaction has a significant impact on understanding drug specificity, metabolism, and absorption. This can be visualized through a fingerprint image depicting the molecular interactions at the protein's active site. The amino acids ASP179, ASN456, SER458 and ASN459 are observed to maintain hydrogen bond with the ligand throughout the simulation period of 100ns, indicating the significance of hydrogen bond having a crucial role in stabilizing the protein-ligand complex. Additionally, during half of the simulation period, the pyridine ring (N3) of the ligand interacts with the LYS318 residue, causing interruptions in its aromacity. Furthermore, hydrophobic interactions involving TRP176 and PHE390 are observed, including  $\pi$ -cation interaction with aromatic group. For almost 94% and 52% of simulation time ASP179 interact with amine group and quinoline nitrogen of ligand through ionic bond and salt bridged interactions, respectively (Fig. 11c). The type of interaction between the ligand and

each catalytic residues of the targeted topoisomerase protein, are responsible for ligand protein stability during the simulation process, was shown with colour coded bar graph (Fig. 11b). In the graph hydrogen, ionic, hydrophobic, and water-brigdged interactions are depicted in green, pink, violet and blue colours, respectively.

#### 4. Conclusion

The study demonstrates the promising potential of the novel quinoline derivative, 6-bromo-N-pyridin-4-yl-2-thiophen-2-ylquinoline-4carboxamide, as a targeted antitumor agent against DNA replicating enzyme. The compound was to have favourable binding affinity to the targeted protein, via molecular docking studies. Further, dynamic simulation results displayed that the ligand - protein complex remained stable over a simulation period of 100ns, and the molecule exhibited a good interaction within active site of targeted protein. The structural conformation of the molecule obtained by single crystal X-ray diffraction revealed the involvement of specific functional groups in intermolecular interactions that contributed to its crystal stability. The study highlights the importance of in silico studies in drug discovery and potential of quinoline derivatives as a template for rational drug design as a viable anticancer agent. Further enhancement in the chemical structure of the compound may provide possible insights into the other potential applications.

# Declaration of generative AI and AI-assisted technologies in the writing process

During the preparation of this work the author(s) used ChatGPT in order to improve the language. After using this tool/service, the author (s) reviewed and edited the content as needed and take(s) full responsibility for the content of the publication.

#### **Supporting information**

CCDC- 2267559 contains the supplementary crystallographic data for this paper. These data can be obtained free of charge via https://www.ccdc.cam.ac.uk/structures/, or by e-mailingdata\_request@ccdc.cam.ac.uk, or by contacting The Cambridge Crystallographic Data Centre, 12 Union Road, Cambridge CB2 1EZ, UK; fax: +44 (0)1223–336.033".

#### CRediT authorship contribution statement

T.S. Shashidhara: Writing – original draft. C.S. Navyashree: Resources, Methodology. M.K. Hema: Conceptualization, Methodology, Resources, Software, Writing – original draft. K. Mantelingu: Methodology. R. Jothi Ramalingam: Software, Formal analysis. Muthusamy Karnan: Software, Formal analysis. M. Umashankar: Methodology. N. K. Lokanath: Supervision, Validation, Writing – review & editing.

#### **Declaration of Competing Interest**

The authors declare that they have no known competing financial interests or personal relationships that could have appeared to influence the work reported in this paper. We declare that, we have no conflict of interest in any direction for the manuscript.

#### Data availability

Data will be made available on request.

#### Acknowledgment

The authors are thankful to National Facility Single Crystal Laboratory, DoS in Physics, Manasagangotri, University of Mysore. Author (R. Jothi Ramalingam) acknowledges Researchers Supporting Project Number (RSP2023R354) King Saud University, Riyadh, Saudi Arabia for funding.

#### Supplementary materials

Supplementary material associated with this article can be found, in the online version, at doi:10.1016/j.molstruc.2023.136266.

# References

- N. Tsomaia, Peptide therapeutics: targeting the undruggable space, Eur. J. Med. Chem. 94 (2015) 459–470.
- [2] N.J. Yang, M.J. Hinner, Getting across the cell membrane: an overview for small molecules, peptides, and proteins, Site Specif. Protein Labeling Methods Protoc. 1266 (2015) 29–53.
- [3] S.L. Schreiber, The small-molecule approach to biology, Chem. Eng. News. 81 (9) (2003) 51–61.
- [4] T. Shiro, T. Fukaya, M. Tobe, The chemistry and biological activity of heterocyclefused quinoline derivatives: a review, Eur. J. Med. Chem. 97 (2015) 397–408.
- [5] 1 M.N. Mustafa, P.A. Channar, M. Sarfraz, A. Saeed, S.A. Ejaz, M. Aziz, A. Hamad, Synthesis, kinetic studies and in-silico investigations of novel quinolinyliminothiazolines as alkaline phosphatase inhibitors, J. Enzyme Inhib. Med. Chem. 38 (1) (2023), 2163394.
- [6] T.A. Wani, S. Zargar, H.M. Alkahtani, N. Altwaijry, L.S Al-Rasheed, Anticancer potential of sulfonamide moieties via *in-vitro* and in-silico approaches: comparative investigations for future drug development, Int. J. Mol. Sci. 24 (9) (2023) 7953.
- [7] T.A. Wani, S. Zargar, Molecular spectroscopy evidence of 1, 3, 5-Tris (4-carboxyphenyl) benzene binding to DNA: anticancer potential along with the comparative binding profile of intercalation via modeling studies, Cells 12 (8) (2023) 1120.
- [8] K.P. Murphy, P.L. Privalov, S.J. Gill, Common features of protein unfolding and dissolution of hydrophobic compounds, Science 247 (4942) (1990) 559–561.
- [9] E. Scott, K. De Paepe, T. Van de Wiele, Postbiotics and their health modulatory biomolecules, Biomolecules 12 (11) (2022) 1640.
- [10] M. Aziz, S.A. Ejaz, S. Zargar, N. Akhtar, A.T. Aborode, T. A. Wani, A.A Akintola, Deep learning and structure-based virtual screening for drug discovery against NEK7: a novel target for the treatment of cancer, Molecules 27 (13) (2022) 4098.

- [11] L. Aramburu, P. Puebla, E. Caballero, M. González, A. Vicente, M. Medarde, R. Peláez, Curr. Med. Chem. 23 (2016) 1100–1130.
- [12] M.F. Mohamed, G.E.D.A. Abuo-Rahma, Molecular targets and anticancer activity of quinoline-chalcone hybrids: literature review, RSC Adv. 10 (52) (2020) 31139–31155.
- [13] S. Jain, V. Chandra, P. Kumar Jain, K. Pathak, D. Pathak, A. Vaidya, Comprehensive review on current developments of quinoline-based anticancer agents, Arabian J. Chem. 12 (8) (2019) 4920–4946.
- [14] D. Duvelleroy, C. Perrio, O. Parisel, M.C. Lasne, Rapid synthesis of quinoline-4-carboxylic acid derivatives from arylimines and 2-substituted acrylates or acrylamides under indium (III) chloride and microwave activations. Scope and limitations of the reaction, Org. Biomol. Chem. 3 (20) (2005) 3794–3804.
- [15] 1468. M. Moutaouakil, S. Tighadouini, Z. M. Almarhoon, M. I. Al-Zaben, A. Ben Bacha, V. H. Masand, R. Saddik, Quinoline derivatives with different functional groups: evaluation of their catecholase activity Catalysts 12 (11) (2022) 1468.
- [16] R. Tabassum, M. Ashfaq, H. Oku, Current pharmaceutical aspects of synthetic quinoline derivatives, Mini Rev. Med. Chem. 21 (2021) 1152–1172.
- [17] D. Insuasty, O. Vidal, A. Bernal, E. Marquez, J. Guzman, Antimicrobial activity of quinoline-based hydroxyimidazolium hybrids, Antibiotics 8 (2019) 239.
- [18] A. Kania, W. Tejchman, A.M. Pawlak, K. Mokrzyński, B. Rózanowski, B. M. Musielak, M. Greczek-Stachura, Preliminary studies of antimicrobial activity of new synthesized hybrids of 2-thiohydantoin and 2-quinolone derivatives activated with blue light, Molecules 27 (2022) 1069.
- [19] O.O. Ajani, K.T. Iyaye, O.T. Ademosun, Recent advances in chemistry and therapeutic potential of functionalized quinoline motifs—A review, RSC Adv. 12 (2022) 18594–18614.
- [20] T.H. Qin, J.C. Liu, J.Y. Zhang, L.X. Tang, Y.N. Ma, R. Yang, Synthesis and biological evaluation of new 2-substituted-4-amino-quinolines and-quinazoline as potential antifungal agents, Bioorganic Med. Chem. Lett. 72 (2022), 128877.
- [21] K.A. Wyman, A.S. Girgis, P.S. Surapaneni, J.M. Moore, N.M. Abo Shama, S. H. Mahmoud, S.S. Panda, Synthesis of potential antiviral agents for SARS-CoV-2 using molecular hybridization approach, Molecules 27 (2022) 5923.
- [22] P.M. Loiseau, K. Balaraman, G. Barratt, S. Pomel, R. Durand, F. Frézard, B. Figadère, The potential of 2-substituted quinolines as antileishmanial drug candidates, Molecules 27 (7) (2022) 2313.
- [23] B. Abdi, M. Fekadu, D. Zeleke, R. Eswaramoorthy, Y. Melaku, Synthesis and evaluation of the antibacterial and antioxidant activities of some novel chloroquinoline analogs, J. Chem. 2021 (2021), 2408006.
- [24] A.M. El-Saghier, M. El-Naggar, A.H.M. Husseinm, A.B.A. El-Adasy, M. Olish, A. H. Abdelmonsef, Eco-friendly synthesis, biological evaluation, and in silico molecular docking approach of some new quinoline derivatives as potential antioxidant and antibacterial agents, Front. Chem. 397 (2021), 679967.
- [25] M.V.V.V. Prasad, R.H.R. Rao, V. Veeranna, V.S. Chennupalli, B. Sathish, Novel quinolone m m derivatives: synthesis and antioxidant activity, Russ. J. Gen. Chem. 91 (2021) 2522–2526.
- [26] K. Govindarao, N. Srinivasan, R. Suresh, R.K. Raheja, S. Annadurai, R.R. Bhandare, A.B. Shaik, Quinoline conjugated 2-azetidinone derivatives as prospective antibreast cancer agents: in vitro antiproliferative and anti-EGFR activities, molecular docking and in-silico drug likeliness studies, J. Saudi Chem. Soc. 26 (3) (2022), 101471
- [27] S. El Rhabori, A. El Aissouq, S. Chtita, F. Khalil, Design of novel quinoline derivatives as anti-breast cancer using 3D-QSAR, molecular docking, and pharmacokinetic investigation, Anticancer Drugs 33 (2022) 789–802.
- [28] C. Verma, M.A. Quraishi, E.E. Ebenso, Quinoline and its derivatives as corrosion inhibitors: a review, Surf. Interfaces 21 (2020), 100634.
- [29] A. Alamiery, Investigations on corrosion inhibitory effect of newly quinoline derivative on mild steel in HCl solution complemented with antibacterial studies, Biointerface Res. Appl. Chem. 2 (2022) 1561–1568.
- [30] G.J. Da Silva Neto, L.R. Silva, Y. Annunciato, Dual quinoline-hybrid compounds with antimalarial activity against Plasmodium falciparum parasites, New J. Chem. 46 (2022) 6502–6518.
- [31] K. Murugan, C. Panneerselvam, J. Subramaniam, M. Paulpandi, R. Rajaganesh, M. Vasanthakumaran, J. Madhavan, S.S. Sha, M. Roni, J.S. Portilla-Pulido, S. C. Mendez, J.E. Duque, L. Wang, A.T. Aziz, B. Chandramohan, D. Dinesh, S. Piramanayagam, J.S. Hwang, Synthesis of new series of quinoline derivatives with insecticidal effects on larval vectors of malaria and dengue diseases, Sci. Rep. 12 (2022) 4765.
- [32] M.V.V.V. Prasad, R.H.R. Rao, V. Veeranna, V.S. Chennupalli, B. Sathish, Novel quinolone derivatives: synthesis and antioxidant activity, Russ. J. Gen. Chem. 91 (2021) 2522–2526.
- [33] D. Gentile, V. Fuochi, A. Rescifina, P.M. Furneri, New anti SARS-CoV-2 targets for quinoline derivatives chloroquine and hydroxychloroquine, Int. J. Mol. Sci. 21 (2020) 5856.
- [34] L. Krstulović, I. Stolić, M. Jukić, T. Opačak-Bernardi, K. Starčević, M. Bajić, I. Glavaš-Obrovac, New quinoline-arylamidine hybrids: synthesis, DNA/RNA binding and tumor activity, Eur. J. Med. Chem. 137 (2017) 196–210.
- [35] Y. Xie, J. Li, Quinoline-based anticancer agents: synthetic approaches and biological activities, ChemMedChem 11 (7) (2016) 731–748.
- [36] M.F.A. Mohamed, GEl-DA. Abuo-Rahma, Molecular targets and anticancer activity of quinoline-chalcone hybrids: literature review, RSC Adv. 10 (52) (2020) 31139–31155.
- [37] R. Nagaraju, et al., Synthesis and anticancer activity of a novel series of tetrazolo [1, 5-a] quinoline based 1, 2, 3-triazole derivatives, Russ. J. Gen. Chem. 90 (2020) 314-318
- [38] C.C.S. Rigaku, Expert 2.0 r15, Software for Data Collection and Processing, Rigaku Corporation, Tokyo, Japan, 2011.

- [39] G.M. Sheldrick, Phase annealing in SHELX-90: direct methods for larger structures, Acta Crystallogr. A 46 (6) (1990) 467–473.
- [40] G.M. Sheldrick, Crystal structure refinement with SHELXL, Acta Crystallogr. C 71 (1) (2015) 3–8.
- [41] O.V. Dolomanov, L.J. Bourhis, R.J. Gildea, J.A. Howard, H. Puschmann, OLEX2: a complete structure solution, refinement and analysis program, J. Appl. Crystal logr. 42 (2) (2009) 339–341.
- [42] A.L. Spek, PLATON, an integrated tool for the analysis of the results of a sin-gle crystal structure determination, Acta Crystallogr. A 46 (s1) (1990) c34. -c34.
- [43] 21 C.F. Macrae, I. Sovago, S.J. Cottrell, P.T. Galek, P. McCabe, E. Pidcock, P. A. Wood, Mercury 4.0: from visualization to analysis, design and prediction, J. Appl. Crystallogr. (2020) 226–235.
- [44] J.J. McKinnon, A.S. Mitchell, M.A. Spackman, Hirshfeld surfaces: a new tool for visualising and exploring molecular crystals, Chemistry 4 (1998) 2136–2141. Easton.
- [45] M.J. Frisch, G.W. Trucks, H.B. Schlegel, G.E. Scuseria, M.A. Robb, J.R. Cheeseman, and D.J. Fox (2016). Gaussian 16.
- [46] R. Dennington, T. Keith, J. Millam, GaussView, Version 6, Semichem Inc., Shawnee Mission, KS, 2009.
- [47] T. Lu, F. Chen, Multiwfn: a multifunctional wavefunction analyzer, J. Comp. Chem. 33 (5) (2012) 580–592.
- [48] W. Humphrey, A. Dalke, K. Schulten, VMD: visual molecular dynamics, J. mol. Graph. 14 (1) (1996) 33–38.
- [49] G.M. Morris, R. Huey, W. Lindstrom, M.F. Sanner, R.K. Belew, D.S. Goodsell, A. J. Olson, Autodock4 and AutoDockTools4: automated docking with selective receptor flexiblity, J. Comput. Chem. 16 (2009) (2009) 2785–2791.
- [50] J. Eberhardt, D. Santos-Martins, A.F. Tillack, S. Forli, AutoDock Vina 1.2. 0: New docking methods, expanded force field, and python bindings, J. Chem. Inf. Model. 61 (8) (2021) 3891–3898.
- [51] O. Trott, A.J. Olson, AutoDock Vina: improving the speedand accuracy of docking with a new scoring function, efficient optimization, and multithreading, J. Comput. Chem. 31 (2) (2010) 455–461.
- [52] D.S. Biovia, Discovery studio visualizer, Discovery studio visualizer 17.20, San Diego, CA, USA, 936.San Diego, 2017.
- [53] Desmond, Schrödinger Release 2023-2: Desmond Molecular Dynamics System, D. E. Shaw Research, New York, NY, 2023. Maestro-Desmond Interoperability Tools, Schrödinger, New York, NY, (2023).
- [54] J. Jayashankar, M.K. Hema, C.S. Karthik, D. Suma, S.R. Kumaraswamy, N. K. Lokanath, P. Mallu, M. Nethaji, N. Lu, Enchant OH··· O interactions in hydrated

- 6-amino-2-methoxypyrimidin-4 (3H) one resembles as water flow in the channel: crystallographic and theoretical investigations, J. Mol. Struct. 1263 (2022), 133098
- [55] M.K. Hema, C.S. Karthik, I. Warad, N.K. Lokanath, A. Zarrouk, K. Kumara, P. Mallu, Regular square planer bis-(4, 4, 4-trifluoro-1-(thiophen-2-yl) butane-1, 3-dione)/ copper (II) complex: trans/cis-DFT isomerization, crystal structure, thermal, solvatochromism, hirshfeld surface and DNA-binding analysis, J. Mol. Struct. 1157 (2018) 69–77.
- [56] T.N. Lohith, M.K. Hema, C.S. Karthik, S. Sandeep, L. Mallesha, P. Mallu, N. K. Lokanath, N-[2-(5-bromo-2-chloro-pyrimidin-4-yl) thio)-4-methoxy-phenyl]-4-chlorobenzenesulfonamide: the existence of H-bond and halogen bond interactions assisted supramolecular architecture—A quantum chemical investigation, J. Mol. Struct. 1267 (2022), 133476.
- [57] M.K. Hema, I. Warad, C.S. Karthik, A. Zarrouk, K. Kumara, K.J. Pampa, N. K. Lokanath, XRD/DFT/HSA-interactions in Cu (II) Cl/phen/B-diketonato complex: physicochemical, solvatochromism, thermal and DNA-binding analysis, J. Mol. Struct. 1210 (2020), 128000.
- [58] K.L. Jyothi, M.K. Hema, K. Kumara, T.G. Row, N.K. Lokanath, Structural elucidation of 1: 4: 4 stochiometric form of thymine–gallic acid cocrystal hydrate: hirshfeld surface analysis, 3D energy framework, DFT calculations, and SARS CoV-2 docking studies, J. Mol. Struct. 1280 (2023), 135072.
- [59] M.K. Hema, C.S. Karthik, K.J. Pampa, P. Mallu, N.K. Lokanath, Solvent induced mononuclear and dinuclear mixed ligand Cu (II) complex: structural diversity, supramolecular packing polymorphism and molecular docking studies, New J. Chem. 44 (41) (2020) 18048–18068.
- [60] T.C. Raveesha, M.K. Hema, K.J. Pampa, P.G. Chandrashekara, K. Mantelingu, T. Demappa, N.K. Lokanath, Analysis of supramolecular self-assembly of two chromene derivatives: synthesis, crystal structure, Hirshfeld surface, quantum computational and molecular docking studies, J. Mol. Struct. 1225 (2021), 129104.
- [61] M.K. Hema, C.S. Karthik, N.K. Lokanath, P. Mallu, A. Zarrouk, K.S. Salih, I. Warad, Synthesis of novel Cubane [Ni4 (O∩ O) 4 (OCH3) 4 (OOH) 4] cluster: xRD/HSAinteractions, spectral, DNA-binding, docking and subsequent thermolysis to NiO nanocrystals, J. Mol. Liq. 315 (2020), 113756.
- [62] S. Nanjundaswamy, M.K. Hema, C.S. Karthik, J.R. Rajabathar, S. Arokiyaraj, N. K. Lokanath, P. Mallu, Synthesis, crystal structure, in-silico ADMET, molecular docking and dynamics simulation studies of thiophene-chalcone analogues, J. Mol. Struct. 1247 (2022), 131365.